JOURNAL OF BACTERIOLOGY, July 1993, p. 4354–4363
0021-9193/93/144354-10$02.00/0

Vol. 175, No. 14

Complete Nucleotide Sequence of the Bacteriophage K1F Tail Gene Encoding Endo-*N*-Acylneuraminidase (Endo-*N*) and Comparison to an Endo-*N* Homolog in Bacteriophage PK1E

JEAN G. PETTER[1]† AND ERIC R. VIMR[1,2]*

Departments of Veterinary Pathobiology[1] and Microbiology,[2] University of Illinois at Urbana-Champaign, Illinois 61801

Received 9 February 1993/Accepted 14 May 1993

Endo-*N*-acylneuraminidase (endo-*N*) is a phage-encoded depolymerase that degrades the α(2-8)-linked polysialic acid chains of K1 serotypes of *Escherichia coli* and vertebrate neural cell adhesion molecules. We have determined the DNA sequence of the bacteriophage K1F tail protein structural gene, which codes for a polypeptide of 920 residues. Purification of the tail protein yields a 102-kDa species upon denaturing gel electrophoresis and detection by Western immunoblot analysis. An identical polypeptide was detected by Western blot analysis of K1F virions. Peptide sequencing confirmed that the open reading frame determined by nucleotide sequencing encodes endo-*N*. Immunoelectron microscopy with neutralizing antibodies raised against the depolymerase confirmed that endo-*N* is a component of the K1F tail apparatus. Antibodies in the serum cross-reacted with endo-*N* from another K1-specific phage, PK1E, demonstrating the presence of shared epitopes. Homology between K1F and PK1E endo-*N* was confirmed by Southern, Northern (RNA), and Western blot analyses. The endo-*N* amino-terminal domain is homologous to the amino termini of phage T7 and T3 tail proteins, indicating by analogy that this domain functions in attachment of endo-*N* to the K1F virion's head. A central domain of 495 residues has weak similarity to sea urchin aryl sulfatase, suggesting that this region may contain the endo-*N* catalytic site. Failure to detect homology between the PK1E homolog and the carboxy-terminal domain of K1F endo-*N* is consistent with the central domain's involvement in binding and catalysis of polysialic acid. These results provide the initial molecular and genetic description of polysialic acid depolymerase, which has so far been detected only in K1-specific phage.

Homopolymeric chains of α2,8-linked sialic acids (polysialic acid [PSA]) are synthesized by certain pathogenic bacteria (reviewed in reference 37) but are more widely distributed on vertebrate N-linked oligosaccharide chains of the neural cell adhesion molecule (NCAM) and sodium channel polypeptide (34, 37). PSA capsules contribute to bacterial invasive potential by the polysaccharide's relatively low immunogenicity and inhibition of complement-mediated killing (37). Although NCAM PSA may modulate homophilic, Ca^{2+}-independent cell-cell adhesion, its primary function in vertebrates may be that of a permissive molecule to regulate other cell-cell interactions by developmentally controlled, spatiotemporal expression of PSA in the embryo and neonate (6, 21, 33–35). Polysialylated NCAM thus qualifies as one of a small set of communicator molecules that appear to regulate tissue morphogenetic pathways (5). Much of the evidence for PSA's postulated morphoregulatory functions comes from perturbation experiments, in which endo-*N*-acylneuraminidase (endo-*N*) is used to selectively shorten PSA chains on NCAM in appropriate developmental systems (33, 35). The structure and genetic organization of this unique PSA depolymerase have not been previously investigated.

Endo-*N* was originally isolated from bacteriophage K1F lysates to facilitate genetic analysis of PSA synthesis in *Escherichia coli* K1 (42, 47, 49, 50). To date, viruses that recognize the K1 capsule as a receptor for infectivity are the only known source of PSA depolymerase (9, 20, 49). As part of our research emphasis on sialic acid metabolism, we carried out an initial molecular characterization of endo-*N* (30). In this communication, we report the complete nucleotide sequence of the endo-*N* structural gene, *g102*, and the derived primary structure of its encoded polypeptide (gp102). The results indicate that endo-*N* is organized into linear domains which are likely to have different functional properties. Comparative analysis of another K1-specific phage, PK1E, indicates homology between K1F and PK1E endo-*N* but not between other sequences in these phage. Thus, except for the common host range specified by endo-*N*, K1F may be no more closely related to PK1E than it is, for example, to T7.

(Portions of this work were presented earlier in preliminary reports [31, 32].)

MATERIALS AND METHODS

Protein purification. The soluble form of endo-*N* was purified from lysates of K1F-infected *E. coli* K1 by a modification of our previously published procedures (12, 49). All manipulations after cell lysis were carried out at 4°C. Lysates were produced by infecting exponentially growing cultures of EV1 or EV36 with 0.1 infectious K1F per cell (12) and then usually concentrated by adding solid ammonium sulfate to 50% saturation. Where indicated, filtration through YM-100 (Amicon) was used as the initial concentration step. Salt-precipitated protein and debris were collected by cen-

* Corresponding author. Electronic mail address: ervimr@ux1.cso.uiuc.edu.

† Present address: Agricultural Research Service, Athens, GA 30605.

trifugation; the pellet was dissolved in 1/100 the initial volume with 10 mM Tris, pH 7.6 (start buffer), and then recentrifuged. The debris pellet was back extracted with an equal volume of start buffer and then added to the initial supernatant. Intact virions were removed by centrifugation at 100,000 × *g*. The concentrated lysate containing soluble endo-*N* was then fractionated by DEAE-Sephacel chromatography with a 600-ml linear gradient of 0 to 0.4 M NaCl in start buffer. Equivalent results were obtained with DEAE-Trisacryl. The column was 2.5 by 20 cm, and 5.5-ml fractions were collected at a flow rate of 0.5 ml min^{-1}. Activity was measured by a substrate depletion assay using colominic acid (Sigma) radiolabeled at its reducing end with sodium borotritide as previously described (12, 43, 49). One unit of endo-*N* produced 1 μg-equivalent of sialic acid in 1 min at 37°C in start buffer. Column fractions were assayed for relative activity from the percentage of substrate counts per minute degraded per unit of time.

Active fractions were pooled, concentrated with ammonium sulfate, dissolved in 2 ml of 50 mM potassium phosphate buffer, pH 7.2, containing 100 mM NaCl, and then dialyzed versus the same buffer. Samples were then usually fractionated by gravity through a column (2.0 by 65 cm) of Sephacryl S-200 at a flow rate of 0.25 ml min^{-1}, although equivalent results were obtained with S-300. Active fractions were again concentrated as described above, redissolved in 10 mM sodium phosphate buffer, pH 6.8, and dialyzed against the same buffer. Enzyme was loaded on a column (1.5 by 15 cm) of hydroxylapatite in the same phosphate buffer. Endo-*N* eluted in the flowthrough, while contaminating proteins were adsorbed. For peptide sequencing, endo-*N* was electroeluted from polyacrylamide after nondenaturing gel electrophoresis as instructed by the manufacturer (Schleicher & Schuell) (30). This purification method has been used successfully by at least two other laboratories (21, 44). Endo-*N* is stable for at least 2 years when stored in 50% glycerol at −20°C.

Gene bank construction and antibody screening. K1F DNA was prepared from CsCl-banded phage particles; other DNA and plasmid manipulations were carried out by the methods given in reference 26. Purified DNA was partially digested to an average size of 1 kb with *Alu*I. The blunt-ended fragments were ligated with oligonucleotide adapters and then cloned into *Eco*RI-derived right and left arms of λgt11 (Promega, Madison, Wis.). Approximately 25% of 8,000 plaques tested had inserts, as judged by blue-white screening on 5-bromo-4-chloro-3-indolyl-β-D-galactoside (X-Gal). Assuming an average insert size of 1 kb and a phage genome size of 38 kb (30), this number of recombinant λgt11 particles represents a potential 50-fold redundancy of the K1F chromosome.

To screen the λgt11 library for endo-*N* epitopes, plaques were lifted to nylon disks, the disks were incubated with a 1:500 dilution of endo-*N* antiserum and epitopes were detected with a horseradish peroxidase-conjugated second antibody (27). Anti-endo-*N* antibodies were produced by subcutaneous injection of a female New Zealand White rabbit with 100 μg of purified endo-*N* in Freund's complete adjuvant. Preimmune serum obtained from the ear vein was negative for anti-endo-*N* antibodies by double-diffusion analysis. At 21 and 35 days after the first injection, the rabbit was boosted with 100-μg samples of endo-*N* injected subcutaneously. A week after the last injection, antiserum was collected, defibrinated, and used without further modification. Screening of the phage DNA library with this antiserum as described above gave 24 positive plaques, of which 9 had unique inserts as determined by subcloning and DNA sequence analysis.

DNA and protein sequencing and computer analysis. DNA sequencing reactions were carried out with double-stranded templates as described previously (16), using Universal forward and reverse primers purchased from U.S. Biochemical (Cleveland, Ohio) or synthetic primers prepared by the University of Illinois Biotechnology Center. Sequencing from intact K1F DNA template was carried out under conditions previously described for λ templates (25), using probe 2 (see below) as the primer. DNA sequences were analyzed with AALIGN and PROSCAN programs in the DNA Star software operated on an IBM PC system. Data bank searches were carried out at the Biotechnology Center's computer station, using a ktup of 2 (23). Jumbled sequence analysis was carried out following the general procedures in Doolittle (7) and statistically analyzed by the procedure given in reference 23.

The N-terminal amino acid sequence of purified endo-*N* was obtained by automated Edman degradation, carried out by the Biotechnology Center Protein Analysis Facility. C-terminal amino acid sequencing was carried out according to Lu et al. (24). Briefly, endo-*N* was dialyzed against water, concentrated with a Centricon 30 (Amicon) microconcentrater, and then diluted to a final concentration of 140 μg in 500 μl of 10 mM sodium acetate, pH 4.0, containing 0.05% (wt/vol) Brij 35 and 50 μg of carboxypeptidase P (Sigma). Time points were taken at 0-, 30-, 40-, and 60-min intervals by bringing 50-μl samples to a final concentration of 10% with 100% trichloroacetic acid. Samples were submitted to the Protein Analysis Facility for amino acid analysis by microbore chromatography (24). Data were expressed as the picomole percentage of each amino acid present per unit of time, after subtracting background levels determined from a zero-time control. Values for each residue detected ranged from 3.5 to 7 pmol% over the 60-min digestion period.

Other analytical procedures. Southern blot analysis was carried out with ^{32}P-labeled, plasmid-derived probes by random priming as described previously (38). Oligonucleotide probes were end labeled as described previously (26). Probe 1 is a plasmid-derived fragment which includes bp 371 to 1306 of the endo-*N* structural gene. Probes 2 (5′-GCGT CAGAGCCGTGCATCAA-3′), 3 (5′-CCAGATGATCGTTA CAAGGC-3′), and 4 (5′-TAGTTGTGAAGGATAATTAC-3′) are oligonucleotides beginning at bp 1735, 1969, and 2120, respectively, of the endo-*N* structural gene. Probe 5 is plasmid derived and includes 109 bp 5′ to the endo-*N* start codon plus 171 bp of the N-terminal coding sequence. Probe 6 is a total *Sau*3A digest of K1F DNA. Colony hybridization was carried out as described previously (16) except that Nytran (Schleicher & Schuell) was used as the support in place of Whatman 541 filter paper. Hybridization and washing conditions for oligonucleotide probes were 10°C below the estimated T_m (26). For Northern (RNA) blot analysis, 5 ml of EV36, at an A_{600} of 0.4, was infected with 10 infective units per cell. After incubation for 5 min at 37°C, 1.5-ml samples were taken in duplicate and total RNA was extracted for agarose electrophoresis and hybridization as described previously (18). RNA standards were purchased from Bethesda Research Laboratories.

Western immunoblot analysis was carried out by the method of Towbin et al. (41). Methods for denaturing polyacrylamide gel electrophoresis in the presence of sodium dodecyl sulfate and the source of prestained molecular weight markers were described previously (17). Proteins were blotted to nitrocellulose, which was incubated with a

TABLE 1. Results of K1F endo-*N* purification

Purification step	Total U	Specific activity (U/mg of protein)	Purification factor	% Recovery
1. Lysate[a]	1,770	1.7	1	100
2. DEAE F-I	231	10.3	6	13
DEAE F-II	60	5.6	3	3
3. S-200 F-I	58	72.0	42	3
S-200 F-II	42	8.3	5	2
4. Hydroxylapatite of F-I	70	700	412	4

[a] The lysate in this experiment was concentrated by ultrafiltration (Materials and Methods). Approximately 50% of the total activity was intact K1F particles.

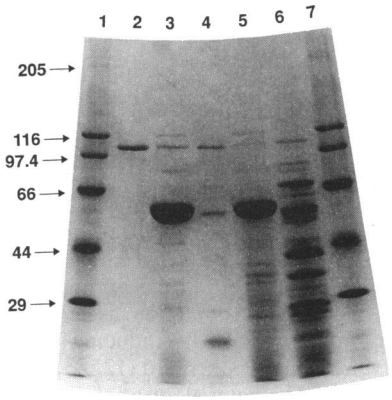

FIG. 1. Electrophoretic analysis of samples taken during endo-*N* purification. Samples from various stages of endo-*N* purification were fractionated by denaturing gel electrophoresis in a 5 to 15% linear acrylamide gradient and then stained with Coomassie blue. Lanes: 1 and 7, molecular weight markers (sizes in kilodaltons are indicated by the numbers at the left); 2, endo-*N* after step 4; 3, F-II after step 3; 4, F-I after step 3; 5, F-II after step 2; 6, F-I after step 2.

1/500 dilution of rabbit antiserum and then with a 1/2,000 dilution of horseradish peroxidase-conjugated goat-anti rabbit immunoglobulin G (IgG), IgM, and IgA (Cappel) for colorimetric detection with 4-chloro-1-naphthol (27).

Hydrophilicity was determined by the algorithm of Hopp and Woods (15), using a window setting of 10. The free energy of formation of the putative RNA hairpin described below was estimated as described by Lewin (22).

The velocity constant, *K*, for phage neutralization by the rabbit antiserum was calculated from the equation $K = (2.3 D/t)(\log p_0/p)$, where p_0 is the number of phage at zero time, p is the number of phage at time t min, and D is the final dilution of serum in the phage-serum mixture (1). *K* values are expressed as the unitless averages of the means ± standard deviations (SD) of four separate determinations each.

Electron microscopy. CsCl-purified K1F particles were suspended in lambda dilution buffer (26) to about 10^{13} PFU ml^{-1} and then incubated overnight at 4°C with 1 volume of water or 1 volume of a 1:1, 1:10, or 1:100 dilution of rabbit endo-*N* antiserum. After these incubations, the phage suspensions were diluted with 0.1 volume of colloidal gold (5 nm)-labeled Cowan I protein A (Jannsen Pharmaceuticals) and then incubated at room temperature for 1 h. To prepare virus for electron microscopy, carbon-coated 2.5% Formvar grids were placed on phage suspensions for 5 min, after which the grids were blotted and stained for 2 min with 2% ammonium molybdate, pH 6.2. The grids were examined at 100 kV in a CX JEOL transmission electron microscope at ×50,000 and ×100,000 magnifications.

Nucleotide sequence accession number. The DNA sequence in this communication has been assigned GenBank accession number M63657.

RESULTS

Purification of soluble endo-*N*. K1F is a rapaciously lytic K1 serotype-specific phage (49) with a latent period of about 15 min at 37°C (46) and an average burst size of 100 PFU. Between 50 and 80% of the total endo-*N* activity remains in the supernatant after centrifugation of lysates under conditions in which >99% of the infectious units are pelleted (49), suggesting that the majority of endo-*N* is not attached to virions at the time of lysis. Endo-*N* remaining in the supernatant is defined as the soluble form of the enzyme. Endo-*N* activity eluted from DEAE-Sephacel in two peaks at 0.15 and 0.2 M NaCl, designated fractions I (F-I) and II (F-II), respectively. As shown in Table 1, F-I contained most of the depolymerase activity. After Sephacryl S-200 chromatography, the specific activity of F-I was greater than that of F-II, which had been chromatographed over a separate S-200 column (Table 1). Further purification of F-II was not attempted; we believe that it is a partially denatured form of the native enzyme in F-I. Differential elution of F-II from DEAE may be due to association with another polypeptide with a monomer molecular weight of 60,000 (Fig. 1, lanes 3 and 5). Transmission electron microscopy of negatively stained F-II revealed a decatetramer with sevenfold rotational symmetry (not shown). Since the GroE holoenzyme has a similar quaternary structure and is composed of subunits with monomer molecular weights of 60,000 (14), it is possible that the 60-kDa band in Fig. 1 (lane 3) represents GroE. No higher-order structures were observed by electron microscopy of F-I or of the purified enzyme. Although the yield of purified endo-*N* after hydroxylapatite chromatography was low (Table 1), replacement of ultrafiltration by concentration with ammonium sulfate at step 1 led to yields of up to 2 mg of endo-*N* from 6 liters of starting lysate. The monomer molecular weight of endo-*N* was estimated as 102,000 (Fig. 1, lane 2).

Characterization of neutralizing antiserum. A 1/5,000 dilution of the rabbit antiserum prepared against purified K1F endo-*N* neutralized infectivity with a velocity constant of 513 ± 25. To determine whether K1F endo-*N* was antigenically related to the depolymerase of another K1-specific phage, the neutralization kinetics with phage PK1E (40) was investigated. Since a 1/2,500 dilution was required to give a velocity constant of 424 ± 44, we conclude that despite reported biochemical differences (28, 29, 40), K1F and PK1E endo-*N* share a subset of identical epitopes and thus are likely to be functionally as well as structurally related.

On the basis of analogy to other phage depolymerases, endo-*N* was assumed to be a component of the viral tail apparatus (12, 49). Direct evidence for this assertion came from cross-linking experiments with anti-endo-*N* antibodies. As shown in Fig. 2A, K1F is a Bradley (2)-type C phage with a spike-like appendage protruding from a unique vertice of the capsid. This spike is surrounded by a hexagonal array of globular structures which we assume are multimers of gp102 (Fig. 2A). Presumably, the spike mediates DNA ejection after binding and degradation of PSA receptors by endo-*N*. That endo-*N* is a component of the tail apparatus was shown

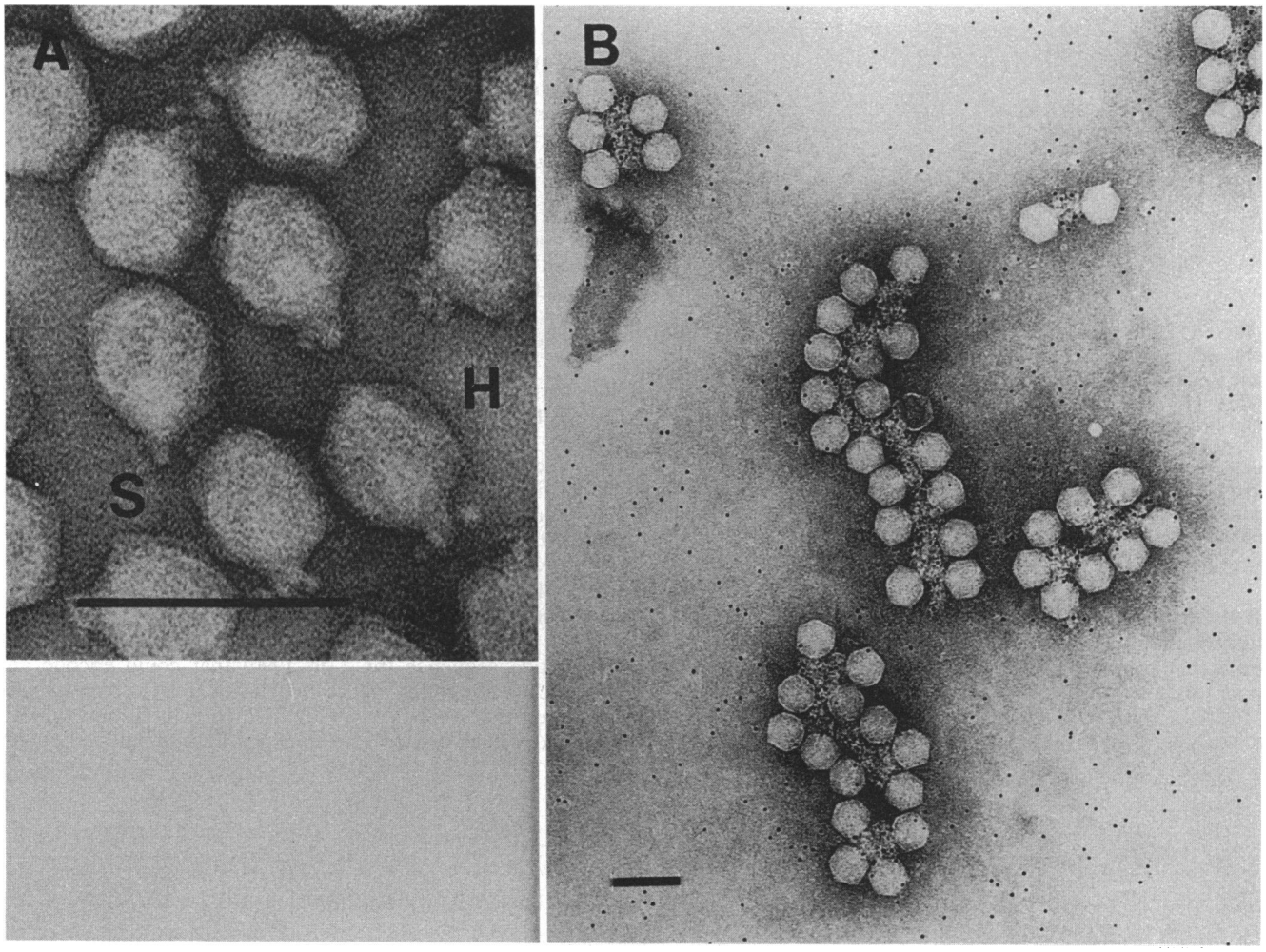

FIG. 2. Transmission electron immunomicroscopy of endo-*N*. (A) Morphology of K1F particles that were not exposed to anti-endo-*N* antibodies. S and H refer to the spike-like projections of K1F virions and the hexagonal arrays, respectively, of endo-*N* structures which are best seen in the particles above these designations. (B) K1F lattices, detected at a 1:10 dilution of anti-endo-*N* antibodies as described in Materials and Methods. Tenfold-lower or -higher dilutions did not yield detectable lattices. Black dots are 5-nm colloidal gold particles linked to protein A. Gold particles are preferentially located in the lattice furrows that were formed by cross-linking K1F particles with anti-endo-*N* antibodies. Bars represent 100 nm.

by the tail-to-tail lattices observed after incubation of K1F with an appropriate dilution of anti-endo-*N* antiserum and secondary gold-labeled protein A, procedures which localized anti-endo-*N* IgG molecules to lattice furrows (Fig. 2B). There were 12 gold particles (±2.2 SD) per 5×10^2 nm^2 of tail lattice furrow, versus a background of 5 ± 2.7 SD ($P < 0.001$). These results strongly suggest that endo-*N* is a component of the virion's tail apparatus.

To demonstrate that neutralizing antibodies recognized endo-*N*, virions were denatured and analyzed by the Western blot technique. Figure 3A shows the Coomassie blue-stained profile of decreasing numbers of K1F (lanes 4 to 9). Purified endo-*N* is shown for comparison in Fig. 3A (lane 3), while an identical sample heated at 37°C instead of 90°C gave a characteristic aggregate that did not enter the separating gel (Fig. 3A, lane 2). Such aggregates are not fully denatured until samples are heated at 55°C (30). When samples containing the same numbers of virions as in Fig. 3A (lanes 6 to 9) were reacted against rabbit antiserum after blotting to nitrocellulose, a band at the position of purified endo-*N* (Fig.

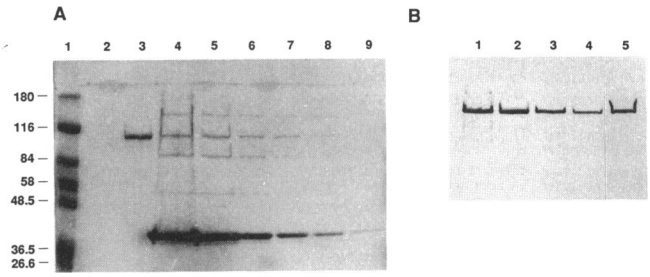

FIG. 3. Western blot analysis of K1F virions. (A) Coomassie blue-stained profile of purified endo-*N* (lanes 2 and 3) and K1F (lanes 4 to 9) fractionated on a denaturing 7.5% separating gel. The stacking gel was 5%. Samples were heated in sample buffer at 90°C prior to electrophoresis except for the sample of endo-*N* in lane 2, which was heated at 37°C. The titers of K1F loaded were 2×10^{11} (lane 4), 1×10^{11} (lane 5), 5×10^{10} (lane 6), 2.5×10^{10} (lane 7), 1.25×10^{10} (lane 8), and 6.25×10^9 (lane 9). Sizes of molecular weight markers (lane 1) are shown in kilodaltons by the numbers at the left. (B) Assay in which K1F, at the same titers as in lanes 6 to 9 in panel A, was blotted to nitrocellulose (lanes 1 to 4, respectively) and probed with rabbit anti-endo-*N* antiserum. Purified endo-*N* is shown in lane 5.

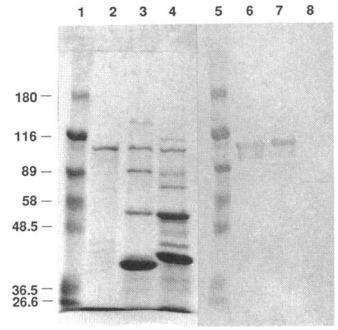

FIG. 4. Evidence that K1F shares epitopes with a 74-kDa polypeptide from PK1E. Approximately 10^{11} K1F (lane 3) or PK1E (lane 4) virions were fractionated by denaturing gel electrophoresis and stained for protein with Coomassie blue. A sample of purified endo-*N* is shown in lane 2. Prestained molecular weight markers are shown in lane 1; their sizes in kilodaltons are indicated by the numbers at the left. Samples identical to those shown in lanes 1 to 4 were blotted to nitrocellulose and incubated with anti-endo-*N* antiserum prior to colorimetric detection of the bound secondary antibody (lanes 5 to 8).

3B, lane 5) was detected (Fig. 3B, lanes 1 to 4). Together with the data in Fig. 2, these results unequivocally demonstrate that soluble endo-*N* is a component of the K1F tail apparatus.

PK1E endo-*N* holoenzyme was reported to be composed of 74- and 38.5-kDa polypeptides (40), suggesting major differences between it and the K1F enzyme (12). Figure 4 shows the electrophoretic profiles of K1F (lane 3) and PK1E (lane 4) virions. Western blot analysis demonstrates that antiserum raised against K1F endo-*N* detects only the 74-kDa species from PK1E (Fig. 4, lane 8). The failure to detect a lower-molecular-weight species suggests that the 38.5-kDa band previously observed in PK1E endo-*N* preparations (40) may be a contaminant. Alternatively, the smaller component may be a subunit of the PK1E tail apparatus that copurifies with endo-*N*. There is no evidence indicating whether both 74- and 38.5-kDa components are required for catalysis. We conclude that K1F and PK1E endo-*N* are antigenically related despite differences in overall molecular weight and possible holoenzyme structures.

DNA sequencing and derived primary structure of endo-*N*. To learn more about the structure of endo-*N*, we initiated efforts to clone the endo-*N* structural gene from K1F DNA. Inserts from positive recombinant phage were subcloned into the *Sma*I site of pUC18 after *Eco*RI overhangs were filled in with T4 polymerase (26). The open reading frame predicted to encode gp102 was confirmed by sequencing the first 29 amino acid residues of purified endo-*N* (Fig. 5). Endo-*N* lacked the predicted N-terminal methionine residue; otherwise the observed peptide sequence, except for one misidentified residue, matched perfectly with the DNA sequence (Fig. 5). These results defined a reading frame in the nucleotide sequence (bp 1 to 1990) that could encode an ~70-kDa polypeptide. Since denaturing gel electrophoresis indicated that endo-*N* was 102 kDa (Fig. 1, 3, and 4), we concluded that fusions encoding the C-terminal portion of

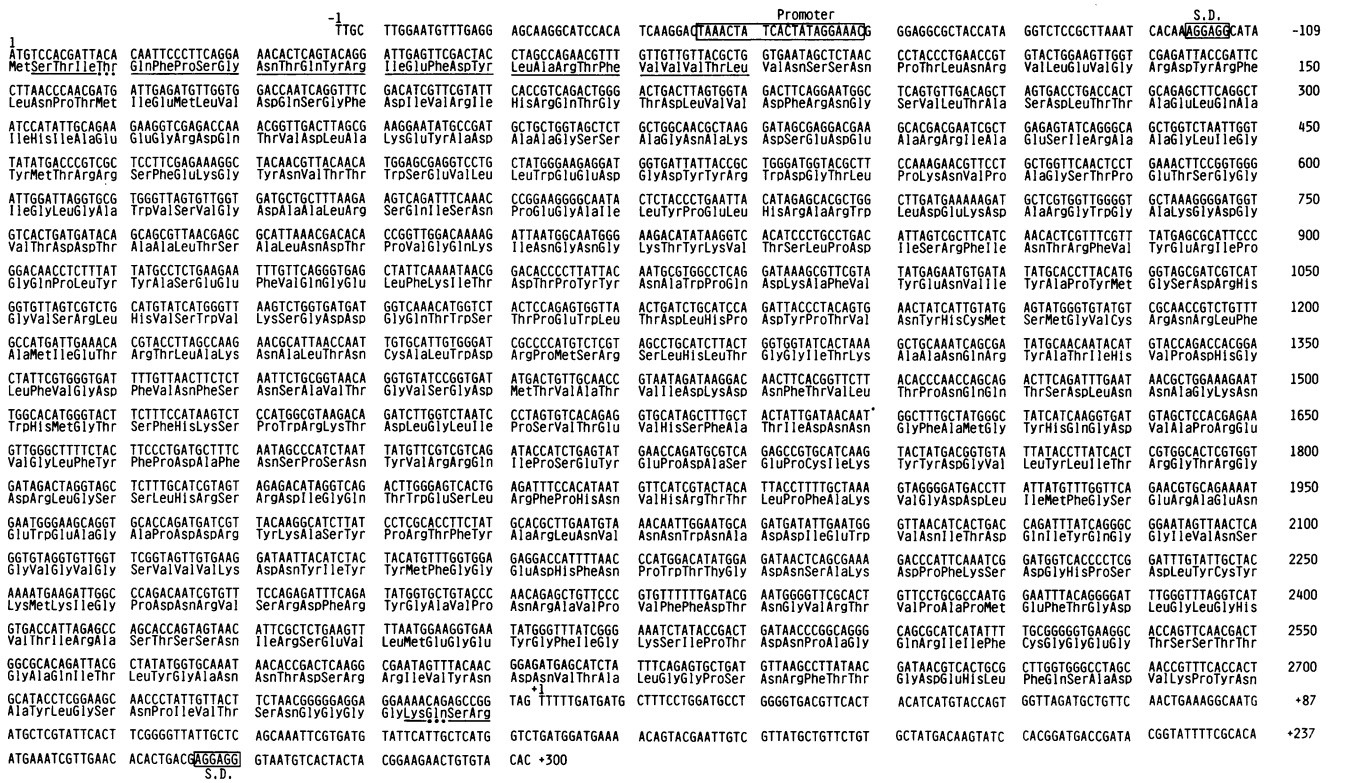

FIG. 5. Nucleotide sequence and genetic organization of *g102* and the derived primary structure of gp102. Endo-*N* structural gene sequences plus 5′ and 3′ noncoding regions are numbered as described in the text. S.D. (Shine-Dalgarno) indicates potential ribosome-binding sites (45) for *g102* and an apparent open reading frame beginning at +276. The potential *g102* promoter is boxed. Underlined amino acid residues represent results of N- and C-terminal peptide sequencing. Dots indicate ambiguous assignments.

the enzyme were not represented in the K1F library or were nonimmunogenic.

Treating K1F DNA with *Sau*3A consistently gave six major digestion products plus numerous apparent partial fragments. We have no completely satisfactory explanation for this incomplete digestion pattern, although the partial fragments may represent differentially modified and thus endonuclease-resistant DNA subpopulations in K1F lysates. One partial *Sau*3A fragment of ~5 kb hybridized weakly to probe 3 but not to probe 2. The size of this fragment indicated that it could contain an end of the phage genome, since g*102* was mapped toward one end of the K1F genome (data not shown). Furthermore, since probe 3 fortuitously contained a *Sau*3A site, we concluded that this partial fragment included one end located in g*102*, plus sufficient downstream DNA to include the 3′ end of g*102*, which apparently was not represented in the K1F genomic library. This fragment was isolated from agarose gels and ligated with *Bam*HI-digested pUC18. Although numerous white colonies were detected on plates containing X-Gal, the resident plasmids in these transformants had suffered deletions into *lacZ* and consequently contained no K1F DNA. Ligation was repeated, and the resulting transformants were subjected to colony hybridization against probe 3. Two positive clones were detected, each of which contained identical 1.6-kb inserts. DNA sequencing demonstrated that the g*102*-distal end of the insert was ligated to vector DNA. We concluded that the K1F-derived partial fragment was ligated at its g*102*-proximal *Sau*3A site into one side of *Bam*HI-digested pUC18 but that either the fragment lacked a second *Sau*3A site or downstream DNA sequences were not tolerated by the recipient. In either case, K1F DNA was apparently excised in vivo, and a shortened religation product was generated by the host bacterium. The possibility that K1F DNA in this region of the genome formed unstable structures would explain the absence of these sequences from our gene library.

DNA sequencing was completed with oligonucleotide primers complementary to g*102* sequences. The complete g*102* sequence could encode a calculated 102,024.1-Da gene product (Fig. 5) with an estimated pI of 5.41, in reasonable agreement with the pI of 5.8 measured by isoelectric focusing of endo-*N* in polyacrylamide gels (48). Further evidence that g*102* encoded endo-*N* came from carboxy-terminal peptide sequencing. Carboxypeptidase P first released Arg, followed by Ser, Glx, and Lys before results could no longer be interpreted. This pattern of amino acid release is consistent with the predicted C-terminal primary sequence derived from nucleotide sequencing (Fig. 5).

Potential control elements in g*102* 5′ and 3′ noncoding regions. As shown in Fig. 5, a typical prokaryotic ribosome-binding site (51) is located 4 bp from the predicted AUG translational start codon of g*102* (bp 1 to 1260). The available upstream sequence (bp −1 to −109) included a putative promoter (Fig. 5) with homology to the consensus sequence of phage promoters recognized by T7 RNA polymerase (8). The potential g*102* promoter is similar to the consensus T7 promoter sequence, especially in the region that is thought to be functionally equivalent with the bacterial Pribnow box (19), strongly suggesting that K1F transcription depends on a phage-specific RNA polymerase. Computer-assisted analysis of the g*102* 3′ noncoding sequence (bp +1 to +300 in Fig. 5) identified two sets of inverted repeats that could form stable hydrogen-bonded secondary structures. The energetically more favorable repeat (−14 kcal [−58.6 kJ]/mol) includes the 53 nucleotides centered around bp +148 (Fig. 5). Since another ribosome-binding site, but no putative promoter, was located 3′ of the inverted repeat, it is likely that g*102* is the first gene transcribed from a K1F operon in which hairpin structures function as *cis* regulatory elements, as previously observed in the T7 system (8). Similarities between the sizes, shapes, and genetic organizations of K1F and T7 thus indicate that these viruses are at least functionally related.

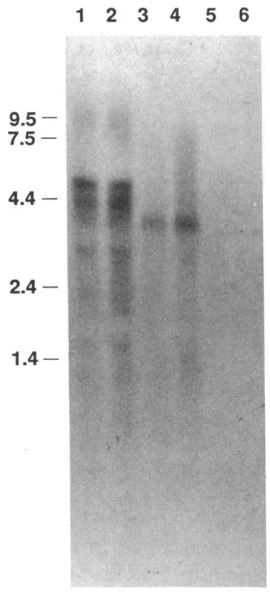

FIG. 6. Evidence that the PK1E homolog of K1F g*102* has a different transcriptional organization. Total RNA from duplicate cultures of EV36 infected with K1F (lanes 1 and 2) or PK1E (lanes 3 and 4) and RNA from uninfected cells (lanes 5 and 6) were extracted for Northern hybridization analysis with probe 1. Numbers at the left indicate the sizes in kilobases of RNA standards.

To support our suppositions about transcriptional organization, total RNA was extracted from K1F-infected cells and subjected to Northern hybridization analysis with probe 1. The signal observed at about 5 kb (Fig. 6, lanes 1 and 2) is consistent with transcription beginning at a g*102* promoter and continuing toward the end of the K1F genome; lower bands may represent breakdown products of this initial multicistronic message. In contrast, RNA from PK1E-infected cells gave one signal at 3.5 kb (Fig. 6, lanes 3 and 4), indicating a transcriptional organization of the PK1E g*102* homolog that is different from K1F's. Cross-hybridization between PK1E mRNA and the K1F-derived probe demonstrates that the antigenic similarity between endo-*N* from these phage extends to homologies at the DNA level.

Domainal organization of endo-*N*. When the derived primary structure of gp102 was queried against all sequences in version 26 of the Protein Identification Resource data bank (10), the first 113 N-terminal amino acid residues matched with a similar N-terminal region of phage T7 and T3 tail proteins. Endo-*N* was 40% identical with gp17 and 60% similar when conservative changes were considered (Fig. 7). Since the comparable domain of gp17 appears to mediate binding of this tail protein to the T7 virion's head (39), we suggest that the homologous region of gp102 may also function in attachment of endo-*N* to the K1F virion. Although the supraquaternary structures of endo-*N* and T7 tail proteins revealed by transmission electron microscopy ap-

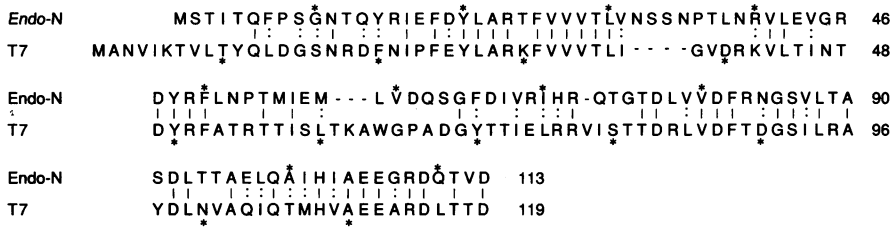

FIG. 7. Homology among N-terminal domains of the tail proteins from phage T3, T7, and K1F. Tail proteins gp102 (endo-*N*) and gp17 (T7) were aligned to maximize identities (vertical lines). Gaps introduced by the computer program are indicated by hyphens. Double dots indicate conservative changes. Numbering is from the N-terminal methionine residues. The tail protein of phage T3 (not shown) is identical to the comparable region of T7 (19).

pear to be quite different (Fig. 2A and reference 39), homologous N-terminal domains are likely to serve similar morphogenetic functions in phage tail assembly.

The N-terminal domain of endo-*N* is separated from successive regions by a glycine-rich potential hinge sequence encoded by bp 595 to 612 (Fig. 5). A similar hinge-like structure has been described in the T7 tail protein (39). Residues 313 to 700 of endo-*N* (Fig. 5) were 8% identical and 25% similar to sea urchin embryo aryl sulfatase (36), with no gaps in the alignment (30). Jumble analysis under different alignment parameters gave *z* scores for the true alignment ranging from 3.7 to 4.2, indicating that the alignment of endo-*N* with aryl sulfatase may be significant. Since both endo-*N* and aryl sulfatase recognize polyanionic substrates, PSA and chondroitin sulfate (36), respectively, the minimal primary sequence similarity may indicate common structural features that are important for the interactions of these enzymes with negatively charged substrates. The hydrophilicity profile of gp102 (not shown) indicates a water-soluble polypeptide, consistent with the behavior of endo-*N* holoenzyme during purification from K1F lysates and its electrophoretic characteristics under nondenaturing conditions (this study; 12, 48).

The central endo-*N* domain is separated from its C-terminal region by a second hinge-like sequence encoded by bp 2101 to 2127 (Fig. 5). This putative domain is apparently not required for catalysis, and it is absent from the PK1E homolog, as shown by hybridization of probe 3 but not probe 4 to restriction digests of PK1E DNA (data not shown). To better define the relationship between K1F and PK1E, DNA was purified from each virus and analyzed by the Southern hybridization technique with K1F-derived probes specific to *g102* sequences or that would detect all K1F DNA sequences. As shown in Fig. 8A (lanes a to f), the *g102*-specific probes 5 and 1 hybridized to restriction fragments containing *g102* sequences. Also as expected, probe 6 detected all K1F sequences (Fig. 8A, lanes g to i). In contrast, probe 6 hybridized to the same set of PK1E restriction fragments (Fig. 8B, lanes g to i) that were detected by the *g102*-specific probes (Fig. 8B, lanes a to f). Therefore, the only sequences with high homology between K1F and PK1E are those encoding endo-*N*. These results indicate that except for the common host range specified by endo-*N*, K1F may be no more closely related to PK1E than it is to T7. Direct sequence comparison with PK1E and other K1-specific phage will be necessary to determine the exact relationships among these phage.

DISCUSSION

The biochemical and molecular characterization of endo-*N* reported in this communication required a simple method for purifying the soluble enzyme. Previous methods either yielded endo-*N* with low activity (40) or involved multiple steps (12). The current method requires only three chromatography steps after cell lysis and yields enzyme of comparable or better electrophoretic purity than that obtained by our previously reported procedures (12, 43). The critical steps in the modified procedure are DEAE chromatography, which removes a partially active fraction, and hydroxylapatite chromatography under conditions in which endo-*N* is not retained by the column. Using these procedures, other workers have also detected F-II (44), although it is not known whether this form of the enzyme is produced before or after cell lysis. The apparent coelution of F-II endo-*N* with GroE suggests that these proteins could be physically associated. Although endo-*N* purified by these procedures appears homogeneous by protein staining. Western blot analysis often reveals a smear of lower-molecular-weight species (30) (Fig. 4, lanes 2 and 6). These species presumably represent proteolytically nicked molecules that can be removed by excising the major band after nondenaturing gel electrophoresis and then subjecting it to electroelution. Although most endo-*N* preparations are stable when stored in 50% glycerol at −20°C, occasional lots develop detectable lower-molecular-weight apparent breakdown products. Consequently, researchers using endo-*N* for in vivo experiments should be aware of possible trace proteolytic and, of course, ubiquitous endotoxin contamination. Sensitive assays exist to assay for endotoxin, while endo-*N* breakdown may be a suitable assay for trace protease activity. These possible complications do not appear to be significant factors in the use of endo-*N* for detection of PSA in complex mixtures (43, 46, 47, 49).

The relatively small size of the K1F genome suggested that cloning of the endo-*N* structural gene would not be technically difficult. However, for reasons that are not entirely clear, we were unable to isolate clones containing sequences much past the 3′ end of *g102* and thus had difficulty in recovering predicted C-terminal coding sequences. The solution to this problem involved a series of fortuitous in vivo cloning events. Our methods of library construction and sequencing thus did not yield any clone containing the intact endo-*N* structural gene, although congruence between the molecular properties of endo-*N* and those predicted by the *g102* open reading frame was supported by N- and C-terminal peptide sequencing. Further confirmation that *g102* encodes endo-*N* came from amplification of *g102* by a polymerase chain reaction using primers complementary to flanking DNA sequences (Fig. 5) and subsequent restriction analysis (3). Work is currently in progress with clones containing the entire endo-*N* open reading frame for anticipated expression studies. Although

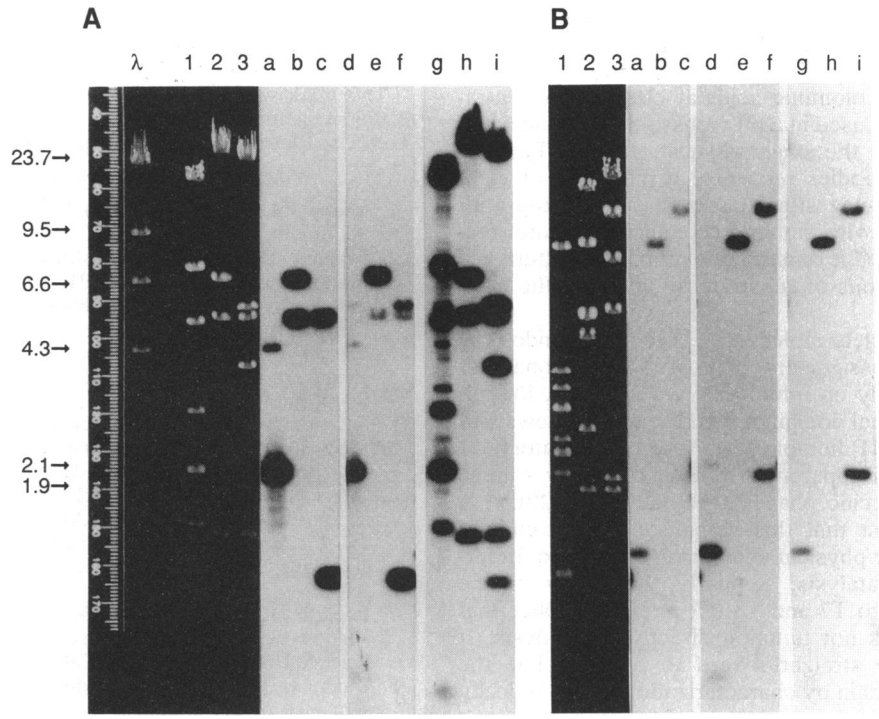

FIG. 8. Evidence that K1F and PK1E genomes share identical endo-*N* coding sequences but are otherwise dissimilar. Purified viral DNA from K1F (A) or PK1E (B) was digested with *Sau*3A (lane 1), *Pvu*II and *Hin*dIII (lane 2), or *Pvu*II and *Bgl*II (lane 3), blotted in triplicate to nylon, and hybridized with probe 5 (lanes a to c), 1 (lanes d to f), or 6 (lanes g to i). λ, phage λ *Hin*dIII markers (sizes in kilobases are given by the numbers at the left).

we detected synthesis of the expected 102-kDa gene product when *g102* was subcloned into an expression vector, we have not yet observed enzymatic activity, indicating post-translational problems such as inclusion body formation or defective folding or oligomerization of endo-*N* (3). In vivo experiments showed that endo-*N* probably does not require any maturative proteolytic processing steps, since no larger-molecular-weight precursors were observed after Western blot analysis of K1F-infected cells (30). Previous results support endo-*N* holoenzyme being a dimer (30–32) or trimer (12) of identical 102-kDa polypeptides.

The possibility that enzymatic activity requires another gene product is unlikely, since highly active preparations contain a single 102-kDa species (this study; 12, 43). While endo-*N* from other K1-specific phage has not been studied in any comparable detail, one report suggests that the PK1E depolymerase is composed of noncovalently associated 74- and 38.5-kDa polypeptides (40). Our results show that neutralizing antiserum raised against purified K1F endo-*N* recognizes the 74-kDa gene product (Fig. 4). While the polyclonal antibodies in this serum effectively inhibit binding of K1F or PK1E to PSA, with velocity constants in the ranges observed for phages T2, T3, T4, T6, and T7 (1), they had little effect on hydrolysis of colominic acid (30), suggesting that PSA-binding and catalytic sites may be separate. Alternatively, the size or spatial organization of PSA on the target cell surface may account for the differential effects of antiserum on binding and catalysis. A recent study of certain host range mutants of PK1E and PK1A suggests that binding and hydrolysis of PSA could be uncoupled (28). Previous studies of certain ε^{15} mutants defective in O-antigen hydrolysis showed that they still bound receptor, although the phage particles were no longer infectious (reviewed in reference 52). Clearly, an understanding of endo-*N* binding and catalysis will require detailed structural information of the sort provided in this communication. Since K1F endo-*N* is being used increasingly for investigating the function of PSA in eukaryotic and prokaryotic systems (reviewed in reference 42), molecular analysis of this depolymerase should also facilitate potentially novel future approaches (45).

Several microbial sialidases (neuraminidases; EC 3.2.1.18) were recently sequenced (reference 16 and references cited therein), and although endo-*N*'s primary structure had no extensive similarity to the primary sequences of these enzymes, both sialidases and endo-*N* were predicted to have a high percentage of β-sheet secondary structure (16, 30). However, unlike sialidases, which cleave terminal sialyl residues from glycoconjugates and polysaccharides, endo-*N* cleaves sialyl residues in, minimally, α2,8-linked sialyl octomers to yield shorter oligomeric products (9, 12, 30, 48, 49). Nuclear magnetic resonance spectroscopy methods indicate that PSA may be a tightly wound helix with ~1-nm pitch, or about four sialyl residues per helical turn (53). Therefore, since an endo-*N* limit digest of PSA produces oligomers ranging in size from three to seven sialyl residues (30), it is likely that the endo-*N* catalytic site is a minimum of 2 nm in length to accommodate an octameric substrate. Earlier reports (12, 29) that high concentrations of endo-*N* cleave substrates smaller than an octomer and may release free sialic acid after long incubation times may be suspect, since trace contamination with exogenous sialidases could account for the observations. Conclusive evidence that endo-*N* recognizes substrates smaller than an octasaccharide awaits controls to unambiguously rule out contamination. Alterna-

tively, different preparative methods may yield endo-*N* with altered substrate specificities. In our hands, incubation of highly purified endo-*N* with defined sialyl dimers through pentamers, or with colominic acid, at enzyme concentrations exceeding those used in a previous study (29) indicated that an octomer was the smallest substrate (30). Furthermore, anti-PSA antibodies recognize a minimum of eight sialyl residues (13), suggesting that both endo-*N* and antibodies may interact with similar secondary structural features of PSA. Knowledge of endo-*N*'s primary structure will aid future investigations of substrate binding and the catalytic mechanism.

Until a more complete molecular dissection of endo-*N* is accomplished, our assignment of possible functional domains is based largely on inference. Nevertheless, the absence of the C-terminal domain in PK1E endo-*N* shows that this region of the K1F homolog may not be obligatory for catalysis. Since it is apparently difficult to purify soluble endo-*N* from K1-specific phage other than K1F (29), it is reasonable to suggest that this domain stabilizes endo-*N* against proteolytic or physical denaturation but is not otherwise involved in catalysis. Similarly, homology of the endo-*N* N terminus to T7 and T3 tail proteins implies that this region also does not function directly in catalysis. It should be relatively straightforward to better define the endo-*N* catalytic domain by characterization of catalytically defective mutants, which appear to arise spontaneously at a detectable frequency (28).

As a component of the phage tail organelle, endo-*N* specificity for PSA defines host range. However, there is no a priori reason that these phage are otherwise related. Indeed, the failure to detect homologous sequences, other than *g102*, between K1F and PK1E implies that these phage are not closely related, a conclusion which is further supported by the different protein profiles and transcriptional organizations of *g102* and its PK1E homolog (Fig. 4 and 6). Convincing evidence has been presented that otherwise unrelated phage may share related tail proteins, indicating horizontal gene transfer and promiscuous illegitimate recombination of the genetic information for tail proteins driven by intense host range selection (11). These observations encourage speculation on the origin of endo-*N*.

Presumably, the evolution of many phage structural genes has an origin in bacteria (4). However, extracts of capsulated and unencapsulated *E. coli* do not degrade PSA, nor has depolymerase activity been detected in vertebrate tissues, which often have high levels of PSA (42, 43, 49). While failure to detect depolymerase other than in phage does not exclude its existence in other sources, it is possible that endo-*N* evolved from extant phage proteins near the time when bacteria evolved PSA. This idea is consistent with evidence that tail genes evolve faster than other phage genes as a result of scrambling of genetic information, leading to highly chimeric tail proteins (11). That the endo-*N* N terminus is homologous with T7 and T3 tail protein N termini (Fig. 7) is consistent with K1F being a part of this phage family, since N-terminal domains interact with other phage proteins and do not change rapidly, while C-terminal domains interact with host receptors and thus have a greater selective pressure to change (11). The central and C-terminal domains of endo-*N* are not homologous to any other known phage tail proteins, nor do *g102* probes hybridize to *E. coli* genomic sequences (30). Additional work is obviously needed to better define the functions of endo-*N* structural domains and to determine the evolution of this unique PSA depolymerase.

ACKNOWLEDGMENTS

We thank E. Basgall for expert assistance with sample preparation and electron microscopy.

This work was supported by research grant AI23039 from the National Institutes of Health. J.G.P. was a predoctoral fellow of the U.S. Department of Agriculture (grant 84-GRAD-9-0062).

REFERENCES

1. **Adams, M. H.** 1959. Bacteriophages, p. 463–464. Interscience Publishers, Inc., New York.
2. **Bradley, D. E.** 1967. Ultrastructure of bacteriophages and bacteriocins. Bacteriol. Rev. **31**:230–314.
3. **Cai, X.-D., D. Stark, U. Rutishauser, J. Petter, and E. R. Vimr.** Unpublished results.
4. **Campbell, A., and D. Botstein.** 1983. Evolution of the lambdoid phages, p. 365–380. *In* R. W. Hendrix, J. W. Roberts, F. W. Stahl, and R. A. Weisberg (ed.), Lambda II. Cold Spring Harbor Laboratory, Cold Spring Harbor, N.Y.
5. **Changeux, J.-P.** 1986. Neuronal man, the biology of mind, p. xiv. Oxford University Press, Oxford.
6. **Doherty, P., and F. S. Walsh.** 1993. Polysialic acid as a specific and positive modulator of NCAM dependent axonal growth, p. 241–255. *In* J. Roth, U. Rutishauser, and F. A. Troy (ed.), Polysialic acid: from microbes to man. Birkhäuser Verlag, Basel.
7. **Doolittle, R. F.** 1986. Of URFs and ORFs, a primer on how to analyze derived amino acid sequences, p. 30–33. University Science Books, Mill Valley, Calif.
8. **Dunn, J. J., and F. W. Studier.** 1983. Complete nucleotide sequence of bacteriophage T7 DNA and the locations of T7 genetic elements. J. Mol. Biol. **166**:477–535.
9. **Finne, J., and P. H. Mäkelä.** 1985. Cleavage of the polysiolosyl units of brain glycoproteins by a bacteriophage endosialidase. Involvement of a long oligosaccharide segment in molecular intervals of polysialic acid. J. Biol. Chem. **260**:1265–1270.
10. **George, D. G., W. C. Barker, and L. T. Hunt.** 1986. The protein identification resource (PIR). Nucleic Acids Res. **14**:11–15.
11. **Haggård-Ljungguist, E., C. Hallig, and R. Calendar.** 1992. DNA sequences of the tail fiber genes of bacteriophage P2: evidence for horizontal transfer of tail fiber genes among unrelated bacteriophages. J. Bacteriol. **174**:1462–1477.
12. **Hallenbeck, P. C., E. R. Vimr, F. Yu, B. Bassler, and F. A. Troy.** 1987. Purification and properties of a bacteriophage-induced endo-N-acetylneuraminidase specific for poly-α-2,8-sialosyl carbohydrate units. J. Biol. Chem. **262**:3553–3561.
13. **Häyrinen, J., D. Bitter-Suermann, and J. Finne.** 1989. Interaction of meningococcal group B monoclonal antibody and its Fab fragment with alpha 2-8-linked sialic acid polymers: requirement of a long oligosaccharide segment for binding. Mol. Immunol. **26**:523–529.
14. **Hendrix, R. W.** 1979. Purification and properties of GroE, a host protein involved in bacteriophage assembly. J. Mol. Biol. **129**: 375–392.
15. **Hopp, T. P., and K. R. Woods.** 1981. Prediction of protein antigenic determinants from amino acid sequences. Proc. Natl. Acad. Sci. USA **78**:3824–3828.
16. **Hoyer, L. L., A. C. Hamilton, S. M. Steenbergen, and E. R. Vimr.** 1992. Cloning, sequencing and distribution of the *Salmonella typhimurium* LT2 sialidase gene, *nanH*, provides evidence for interspecies gene transfer. Mol. Microbiol. **6**:873–884.
17. **Hoyer, L. L., P. Roggentin, R. Schauer, and E. R. Vimr.** 1991. Purification and properties of cloned *Salmonella typhimurium* LT2 sialidase with virus-typical kinetic preference for sialyl α2→3 linkages. J. Biochem. **110**:462–467.
18. **Kornblum, J. S., S. J. Projan, S. L. Moghazeh, and R. P. Novick.** 1988. A rapid method to quantitate non-labeled RNA species in bacterial cells. Gene **63**:75–85.
19. **Krüger, D. H., and C. Schroeder.** 1981. Bacteriophage T3 and bacteriophage T7 virus-host cell interactions. Microbiol. Rev. **45**:9–51.
20. **Kwiatkowski, B., B. Boschek, H. Thiele, and S. Stirm.** 1983. Substrate specificity of two bacteriophage-associated endo-*N*-acetylneuraminidases. J. Virol. **45**:367–375.

21. **Landmesser, L., L. Dahm, J. Tang, and U. Rutishauser.** 1990. Polysialic acid as a regulator of intramuscular nerve branching during embryonic development. Neuron **6**:655–667.
22. **Lewin, B.** 1987. Genes, p. 62. John Wiley & Sons, New York.
23. **Lipman, D. J., and W. R. Pearson.** 1985. Rapid and sensitive protein similarity searches. Science **227**:1435–1441.
24. **Lu, H. S., M. L. Klein, and P.-H. Lai.** 1988. Narrow-bore high-performance liquid chromatography of phenylthiocarbamoyl amino acids and carboxypeptidase P digestion for protein C-terminal sequence analysis. J. Chromatogr. **447**:351–364.
25. **Manfioletti, G., and C. Schneider.** 1988. A new and fast method for preparing high quality lambda DNA suitable for sequencing. Nucleic Acids Res. **16**:2873–2884.
26. **Maniatis, T., E. F. Fritsch, and J. Sambrook.** 1982. Molecular cloning: a laboratory manual. Cold Spring Harbor Laboratory, Cold Spring Harbor, N.Y.
27. **Mierendorf, R. C., C. Percy, and R. A. Young.** 1987. Gene isolation by screening λgt11 libraries with antibodies. Methods Enzymol. **152**:458–469.
28. **Pelkonen, S., J. Aalto, and J. Finne.** 1992. Differential activities of bacteriophage depolymerase on bacterial polysaccharide: binding is essential but degradation is inhibitory in phage infection of K1-defective *Escherichia coli*. J. Bacteriol. **174**: 7757–7761.
29. **Pelkonen, S., J. Pelkonen, and J. Finne.** 1989. Common cleavage pattern of polysialic acid by bacteriophage endosialidases of different properties and origin. J. Virol. **63**:4409–4416.
30. **Petter, J. G.** 1991. Ph.D. thesis. University of Illinois, Urbana.
31. **Petter, J. G., and E. R. Vimr.** 1988. Purification, characterization, and cloning of bacteriophage K1F endoneuraminidase, abstr. M-4, p. 123. Abstr. 88th Annu. Meet. Am. Soc. Microbiol. 1988.
32. **Petter, J. G., and E. R. Vimr.** 1989. Characterization and sequencing of bacteriophage K1F endoneuraminidase, abstr. M-9, p. 124. Abstr. 89th Annu. Meet. Am. Soc. Microbiol. 1989.
33. **Rutishauser, U., A. Acheson, A. K. Hall, D. M. Mann, and J. Sunshine.** 1988. The neural cell adhesion molecule (NCAM) as a regulator of cell-cell interactions. Science **240**:53–57.
34. **Rutishauser, U., and T. M. Jessell.** 1988. Cell adhesion molecules in vertebrate neural development. Physiol. Rev. **68**:819–857.
35. **Rutishauser, U., M. Watanabe, J. Silver, F. A. Troy, and E. R. Vimr.** 1985. Specific alteration of NCAM-mediated cell adhesion by an endoneuraminidase. J. Cell Biol. **101**:1842–1849.
36. **Sasaki, H., K. Yamada, K. Akasaka, H. Kawasaki, K. Suzuki, A. Saito, M. Sato, and H. Shimada.** 1988. cDNA cloning, nucleotide sequence and expression of the gene for arylsulfatase in the sea urchin (*Hemicentrotus pulcherrimus*) embryo. Eur. J. Biochem. **177**:9–13.
37. **Silver, R. P., and E. R. Vimr.** 1990. Polysialic acid capsule of *Escherichia coli* K1, p. 39–60. *In* B. Iglewski and V. Miller (ed.), The bacteria, vol. 11. Molecular basis of bacterial pathogenesis. Academic Press, Inc., New York.
38. **Steenbergen, S. M., and E. R. Vimr.** 1990. Mechanism of polysialic acid chain elongation in *Escherichia coli* K1. Mol. Microbiol. **4**:603–611.
39. **Steven, A. C., B. L. Trus, J. V. Maizel, M. Unser, D. A. D. Parry, J. S. Wall, J. F. Hainfeld, and F. W. Studier.** 1988. Molecular substructure of a viral receptor-recognition protein. The gp17 tail-fiber of bacteriophage T7. J. Mol. Biol. **200**:351–365.
40. **Tomlinson, S., and P. W. Taylor.** 1985. Neuraminidase associated with coliphage E that specifically depolymerizes the *Escherichia coli* K1 capsular polysaccharide. J. Virol. **55**:374–378.
41. **Towbin, H., T. Staehelin, and J. Gordon.** 1979. Electrophoretic transfer of proteins from polyacrylamide gels to nitrocellulose sheets: procedure and some applications. Proc. Natl. Acad. Sci. USA **76**:4350–4354.
42. **Troy, F. A.** 1992. Polysialylation: from bacteria to brains. Glycobiology **2**:5–23.
43. **Troy, F. A., P. C. Hallenbeck, R. D. McCoy, and E. R. Vimr.** 1986. Detection of polysialosyl-containing glycoproteins in brain using prokaryotic-derived probes. Methods Enzymol. **138**:169–185.
44. **Vann, W. F.** Personal communication.
45. **Varki, A., F. Hooshmand, S. Diaz, N. M. Varki, and S. M. Hedrick.** 1991. Developmental abnormalities in transgenic mice expressing a sialic acid-specific 9-O-acetylesterase. Cell **65**:65–74.
46. **Vimr, E. R.** 1992. Selective synthesis and labeling of the polysialic acid capsule in *Escherichia coli* K1 strains with mutations in *nanA* and *neuB*. J. Bacteriol. **174**:6191–6197.
47. **Vimr, E. R., W. Aaronson, and R. P. Silver.** 1989. Genetic analysis of chromosomal mutations in the polysialic acid gene cluster of *Escherichia coli* K1. J. Bacteriol. **172**:1106–1117.
48. **Vimr, E. R., and E. J. Basgall.** 1986. Development of coliphage K1F endoneuraminidase for detection and selective modification of polysialic acid in neural glycoconjugates. Fed. Proc. **45**:1815.
49. **Vimr, E. R., R. D. McCoy, H. F. Vollger, N. C. Wilkison, and F. A. Troy.** 1984. Use of prokaryotic-derived probes to identify poly(sialic acid) in neonatal neuronal membranes. Proc. Natl. Acad. Sci. USA **81**:1971–1975.
50. **Vimr, R. E., and F. A. Troy.** 1985. Regulation of sialic acid metabolism in *Escherichia coli*: role of *N*-acylneuraminate pyruvate-lyase. J. Bacteriol. **164**:845–853.
51. **von Heijne, B.** 1987. Sequence analysis in molecular biology. Treasure trove or trivial pursuit, p. 44–49. Academic Press, San Diego, Calif.
52. **Wright, A., M. McConnell, and S. Kanegasaki.** 1980. Lipolysaccharide as a bacteriophage receptor, p. 28–57. *In* L. L. Randall and L. Philipson (ed.), Virus receptors, part 1. Bacterial viruses, series B, vol. 7. Chapman & Hall, London.
53. **Yamasaki, R., and B. E. Bacon.** 1991. Three-dimensional structural analysis of the group B polysaccharide of *Neisseria meningitidis* 6275 by two-dimensional NMR: the polysaccharide is suggested to exist in helical conformations in solution. Biochemistry **30**:851–857.